Transplant International ISSN 0934-0874

ORIGINAL ARTICLE

In vivo magnetic resonance imaging of vascularization in islet transplantation

Eba Hathout,[1] Lawrence Sowers,[1] Rong Wang,[2] Annie Tan,[1] John Mace,[1] Ricardo Peverini,[1] Richard Chinnock[1] and Andre Obenaus[2]

1 Islet Transplant Laboratory, Departments of Pediatrics, Loma Linda University School of Medicine, CA, USA
2 Radiation Medicine, Loma Linda University School of Medicine, CA, USA

Keywords
imaging, islet transplant, islet vascularization.

Correspondence
Eba Hathout, MD, Prof. and Chief, Division of Pediatric Endocrinology, and Director, Pediatric Diabetes Center and Islet Transplant Laboratory, Department of Pediatrics, Loma Linda University School of Medicine, 11175 Campus Street, Coleman Pavilion, A1120R, Loma Linda, CA 92354, USA. Tel.: +1 909 558 4130; fax: +1 909 558 0408; e-mail: ehathout@llu.edu

Received: 6 July 2007
Revision requested: 18 July 2007
Accepted: 3 August 2007

doi:10.1111/j.1432-2277.2007.00550.x

Summary

To evaluate changes in neovascularization of transplanted islets *in vivo*, dynamic contrast (gadolinium) enhanced magnetic resonance imaging (MRI) was used. Both iron (Feridex)-labeled and unlabeled syngeneic murine subcapsular islet grafts were studied. Differences in dynamic contrast enhancement of islet grafts were quantified after gadolinium injection at post-transplant days 3 and 14. Normalized contrast concentrations at day 14 in transplanted islets were increased relative with that on day 3. Time to peak contrast enhancement was faster by 12 min at day 14 compared to day 3 islets (while kidney and muscle peak times remained the same). Areas under the curve for contrast concentration versus time plots were larger in 14-day relative to 3-day islet grafts. In conclusion, noninvasive assessment of neovascularization is achievable. *In vivo* dynamic contrast-enhanced MRI can be used to detect and quantify changes in vascularization following islet transplantation. This technique may be useful in developing pro-angiogenic strategies to improve the transplantation outcome in experimental and clinical settings.

A main challenge for long-term insulin-independence following islet transplantation in type 1 diabetes is occult hypoxic, inflammatory, and immune graft loss [1–3]. Anoxia from initial avascularity is particularly stressful to islets function in the hyperglycemic milieu of a diabetic recipient [4,5]. Therefore, monitoring and improving early vascularization of islet grafts is pivotal for their long-term viability and function in both experimental and clinical settings.

Although microscopy provides high spatial-resolution images of preserved tissue, clinically facile methods are needed to image viable islet grafts *in situ*. Several studies have confirmed the ability to localize islets by magnetic resonance imaging (MRI) both *in vitro* and *in vivo* [6–10]. Other imaging modalities, such as positron emission tomography using 18-fluro-deoxyglucose, can also visualize islet location but suffer from short half-lives and poor resolution, favoring MR contrast as a high-resolution method. [11].

Dynamic contrast-enhanced (DCE) MRI is an imaging modality that can noninvasively measure key hemodynamic parameters such as blood flow, blood volume, interstitial volume, and capillary permeability in real time. The method has been used experimentally and clinically to assess the tumor angiogenesis and develop the anticancer drugs [12–16]. DCE MRI has also been used to evaluate the angiogenesis of tissue-engineered bladders [17] and to test the response to vascular endothelial growth factor therapy [18].

We previously reported that a significant increase in islet vascularization follows a rise in hypoxia-inducible factor-1α in islet grafts, and that development of newly formed microvessels is more abundant on post-transplant day 14 in comparison to day 3 [19].To understand better the time-course of vascularization of islet grafts, and its relation with function, an accurate and reproducible method of imaging islet revascularization *in vivo* is needed. To our knowledge, this is the first published

work on the use of DCE MRI to evaluate vascularization in islet transplantation to date. In this study, we demonstrate that this temporal evolution of neovascularization in islet grafts can be detected by contrast-enhanced MRI.

Research design and methods

Animals

Adult Balb/c mice weighing 25–30 g were purchased (Harlan, Indianapolis, IN, USA) and housed under specific pathogen-free conditions with a 12-h light/dark cycle and had free access to food and water. The Institutional Animal Care Use Committee approved the experimental protocol.

Islet transplantation studies

Islets were isolated by collagenase digestion of the pancreas and Ficoll density gradient centrifugation and then hand-picked [20]. Four hundred syngeneic islets were transplanted under the kidney capsule of normal recipients.

Islet labeling

Iron labeling of islets was performed by overnight co-culture of freshly isolated islets in Feridex (Advanced Magnetics Inc., Cambridge, MA, USA)-supplemented medium at 200 μg iron/ml as described [6].

MRI

Mice were lightly anesthetized using isoflurane (3% induction and 1% maintenance). A tail vein catheter was inserted and fastened to the tail for infusion of gadolinium DTPA (Gd-DTPA,-BMA, Gadodiamide, 0.1 mmol/kg body weight, Omniscan, Amersham Health, Princeton, NJ, USA) contrast. Body temperature was maintained at 36 ± 1 °C using a thermostat-controlled heated water cushion placed under the mouse. Respiration was monitored with an MR-compatible pressure transducer on a Biopac MP150 (Goleta, CA, USA) system. MRI data were collected on a Bruker Advance 11.7 T MRI (8.9-cm bore) with a 3.0 cm (ID) volume radiofrequency coil (Bruker Biospin, Billerica, MA, USA). Scout images were obtained in the axial, sagittal, and coronal planes to position slices accurately. Specifically, the imaging parameters were as follows. 10 echo T2 sequence with a TR/TE of 4600/10 ms, a 128 matrix, a 3-cm field of view (FOV), two averages for a total acquisition time of 20 min. The pre/postcontrast T1 was composed of a TR/TE of 832/10 ms, a 256 matrix, 3-cm FOV, and two averages for a total acquisition time of 14 min. The standard T2 and T1 sequences collected 20 coronal slices that were 0.75-mm thick and interleaved by 0.75 mm. The DCE sequence was a rapid image acquisition that acquired one image slice through the kidney at the level of the islets with the following parameters: TR/TE = 250/10 ms, 64 matrix, 3-cm FOV, one average for an acquisition time of 16 s/image and a total acquisition time of 32 min with 120 images collected. The entire MRI data collection period lasted about 100 min.

MRI analysis

All T2 and T1 image data sets were visually evaluated to identify the location of transplanted islets within each animal. The DCE acquisition slice was then placed over the region of maximal volume of transplanted islets. Beyond visual inspection of imaging, quantitative evaluation of MR parameters was undertaken. This included: (i) calculation of islet volume, (ii) mapping T2 values in the transplanted islets, muscle and kidney, and (iii) DCE analysis for temporal changes in vascularization in three tissue regions (islets, muscle, and kidney).

Islet volume

Transplanted islet volume was calculated by obtaining the area on each T2 and T1 imaging slice and then calculating the total islet volume using CHESHIRE software (Parexcel, International Corp., Waltham, MA, USA).

T2 relaxation values

Islet T2 relaxation times were extracted from T2 maps calculated using an in-house MATLAB program to calculate a pixel-by-pixel T2 map, as previously described [21]. T2 relaxation regions of interest (ROI) analysis was performed on a single image from the data set in islets, kidney and muscle and results were summarized in a spreadsheet and reported as mean ± SEM for the total cohort.

DCE analysis

Temporal change of signal intensity was visualized and quantified using JIM software (Thorpe, Waterville, UK). ROIs (islet, muscle, and kidney) were outlined on the DCE data based on T1 and T2 high resolution images. Kinetic analysis used a bidirectional two-compartment model based on the equations of Tofts *et al.* [22]. All signal intensities were converted to (Gd) values by averaging precontrast R1 (1/T1), and assuming that:

$$R1 = R1pre + \rho(Gd),$$

where $\rho = 1$ as we assumed that there was no difference between plasma relaxivity (relaxivity of the contrast agent

in plasma) and interstitial relaxivity (relaxivity of the contrast agent in the extra-vascular extra-cellular space) and R1pre is the average precontrast R1.

In the standard Tofts model, the tissue (Gd), C_t (t) is related to the plasma (Gd), C_p (t) by:

$$C_t(t) = K_{trans} \int_0^t C_p(t)\exp(-K_{trans}(t-T)/v_e)dT,$$

where v_e is the extra-vascular extra-cellular space volume fraction. This model neglects any contribution to the signal intensity of the passing contrast in intact blood vessels within the tissue of interest. The arterial input function was defined from the abdominal aorta that was visible within the slice of interest. DCE analysis using the Tofts model yields estimates of constants such as the transfer constant (K_{trans}), the extravascular extracellular space fractional volume (v_e), and a measure of the goodness of fit. DCE MRI tissue Gd concentration curves extracted from JIM software were normalized for inter- and intra-animal comparisons.

Selected time-points for imaging

In our previously published data to evaluate the temporal progression of neovascularization in islet grafts prior to MRI, we assessed subcapsular islet grafts on post-transplant days 3, 7, and 14 by optical microscopy [19,20]. Over the course of this experimental period, there was a progressive increase in blood vessel formation. Others have shown that islet graft vascularization is complete by day 14. Based on the above information, days 3 and 14 were selected as two representative time points for the detection of neovascularization (immature and advanced, respectively) in transplanted islets using DCE MRI.

Statistical analysis

Statistical evaluation was performed using SIGMASTAT software (SPPS, Chicago, IL, USA) and differences among experimental groups were considered significant for $P < 0.05$. Data were expressed as the mean ± SE of the mean (SEM).

Results

Quantitative MR analysis of transplanted islets

Feridex-labeled islets could be seen under the kidney capsule as distinct hypointense regions on day 3 and 14 (Fig. 1a). Islet volume was not significantly different between day 3 and day 14 (Fig. 1b). T2 values in three ROIs, islets, muscle, and kidney, were evaluated. Within the transplanted islets, no significant differences were observed between day 3 (122.9 ± 18.8 ms) and day 14 (125.8 ± 24.5 ms). Similarly, muscle (63.3 ± 1.6 vs. 65.3 ± 2.0 ms) and kidney (75.1 ± 5.2 vs. 73.9 ± 2.4 ms) T2 values remained unaltered between day 3 and day 14. However, within the day three experimental period, there was a significant difference in islet T2 values (123 ± 38 ms) compared to T2 values of muscle (63 ± 3 ms) and kidney (75 ± 10 ms, $P < 0.05$). At day 14, islet T2 values were not significantly elevated when compared to kidney ($P < 0.08$), but was significantly increased when compared to muscle ($P < 0.05$). There were no significant differences between muscle and kidney at any time point (Fig. 1c).

Contrast-enhanced imaging of unlabeled and labeled islet grafts

Unlabeled islets

Standard T1-weighted imaging (T1WI; pre- and postcontrast) was undertaken to determine the location of the transplanted islets ($n = 10$ mice). In T1WI without contrast, there was no visible transplanted tissue in any of the animals imaged at days 3 or 14. However, injection of the T1 contrast agent, gadolinium DTPA (0.6 ml/kg), allowed visualization of signal enhancement in every case of subcapsular islet transplantation at day 3 and at day 14 animals.

Labeled islets

To check if microscopically observed blood vessels in islet grafts on day 14 could be detected *in vivo*, contrast imaging of iron-labeled islet grafts was performed ($n = 4$, one graft per recipient). Postcontrast MRI at day 14 clearly showed blood vessels (Fig. 2a and b) in the vicinity of the transplanted islets, with no similar findings in the contralateral kidneys. The relationship between transplanted islets and newly formed blood vessels was further examined by macroscopic photography of the transplanted islets and kidney (Fig. 2c).

DCE MRI of islet grafts

Dynamic contrast-enhanced MRI was undertaken to determine the feasibility of *in vivo* imaging of microscopically detected increased islet graft vascularization between day 3 and day 14. A group of four animals underwent DCE MR imaging to determine the relationship between vessel formation and contrast enhancement within transplanted islets. High-resolution precontrast images were obtained prior to DCE MRI to assist in localization of the ROIs (transplanted islets, muscle, and kidney). DCE MR imaging was started and a bolus of contrast (Gd-DTPA, 0.6 ml/kg) was injected 2 min after the onset of imaging. There was an incremental increase

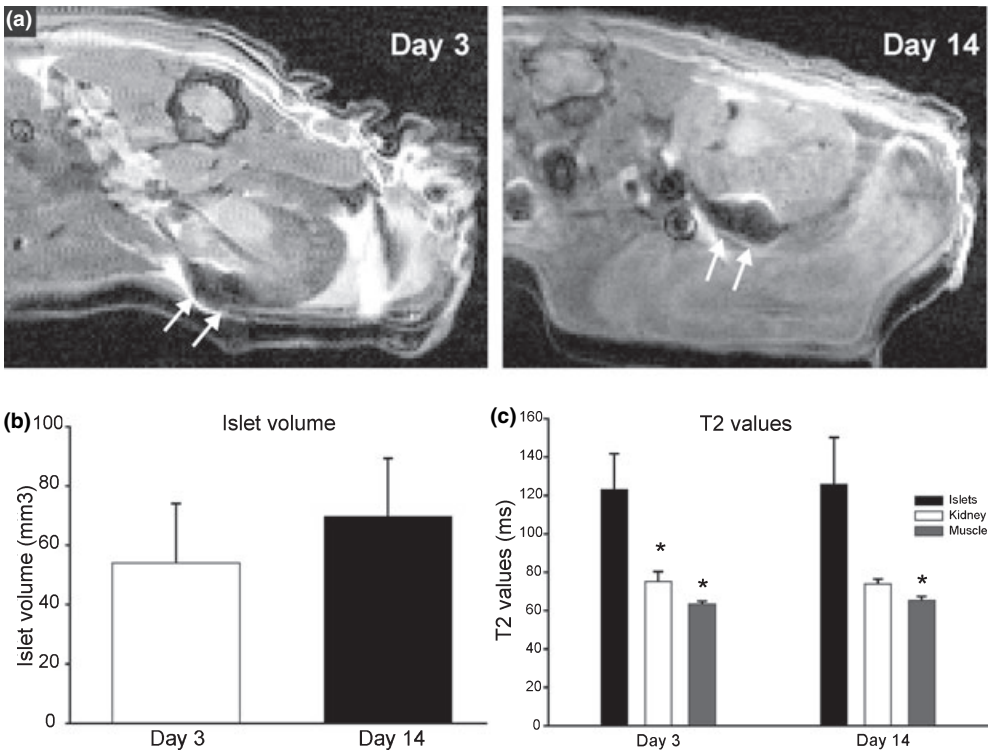

Figure 1 Temporal imaging of iron-labeled islets. (a) T2-weighted image at day 3 and day 14 illustrate that iron-labeled islets can be visualized (loss of signal, arrow) after implantation. (b) Volumetric analysis of the implanted islets demonstrates an unchanged islet mass with time post-transplantation. $*P > 0.05$, $n = 4$. (c) Quantitative evaluation of T2 values from islets shows no change with time post-transplantation. $*P > 0.05$, $n = 4$.

in contrast within the tissues over the course of the 30-min evaluation period.

Quantification of the temporal increase in contrast enhancement was undertaken (Fig. 3). There was a gradual increase in gadolinium tissue concentration within the islets at day 3 over the course of the 30-min DCE experiment (Fig. 3a). In islet day 3 datasets, the time to maximal relative tissue concentration of contrast was 21.40 min (1284.02 ± 187.61 s). There was a slow continuous rise in contrast concentration over the 30-min observation period, which then reached a plateau. In the day 14 animals, gadolinium concentration reached a peak at 9.77 min (586.30 ± 24.06 s), which was significantly shorter than day 3 ($P < 0.01$). The time to peak in muscle and kidney at day 3 was significantly shorter than islets ($P < 0.05$). There was no significant difference within muscle or kidney in time to peak at either day 3 or day 14 (ANOVA). In day 14 transplanted islets, maximal tissue concentration was observed 11.63 min earlier than in day 3 islets (Fig. 3a). In addition, the normalized maximal tissue concentration in islets was 1.04 at day 3 compared to 1.63 at day 14, representing a 57% increase in gadolinium tissue concentration. The area under the curve of the islet DCE MRI datasets (Fig. 3a) was also 62% larger at day 14 compared to day 3 ($P < 0.05$, Fig. 3b).

Discussion

This study builds on the work of many others who have already unequivocally demonstrated that Feridex labeling of islet grafts is specific, safe, and effective for their localization by MRI [23–25]. To achieve direct visualization of transplanted islets by MRI, iron labeling of isolated islets before transplantation seemed to be a logical method to facilitate detection and tracking of the islet grafts. The methodology of iron labeling in pancreatic islets has been formally addressed by Evgenov *et al.* [6,23] and Kriz *et al.* [24]. In this study, we similarly showed that *in vitro* iron labeling of islets resulted in precise localization of islet grafts characterized by robust hypointensities on day 3 and day 14. To our knowledge, ours is the first demonstration of non-invasive *in vivo* imaging of changes in vascularization following islet transplantation using DCE MRI. In this study, we showed in an experimental islet transplant setting that changes in vascularization could be quantified *in vivo* via this approach.

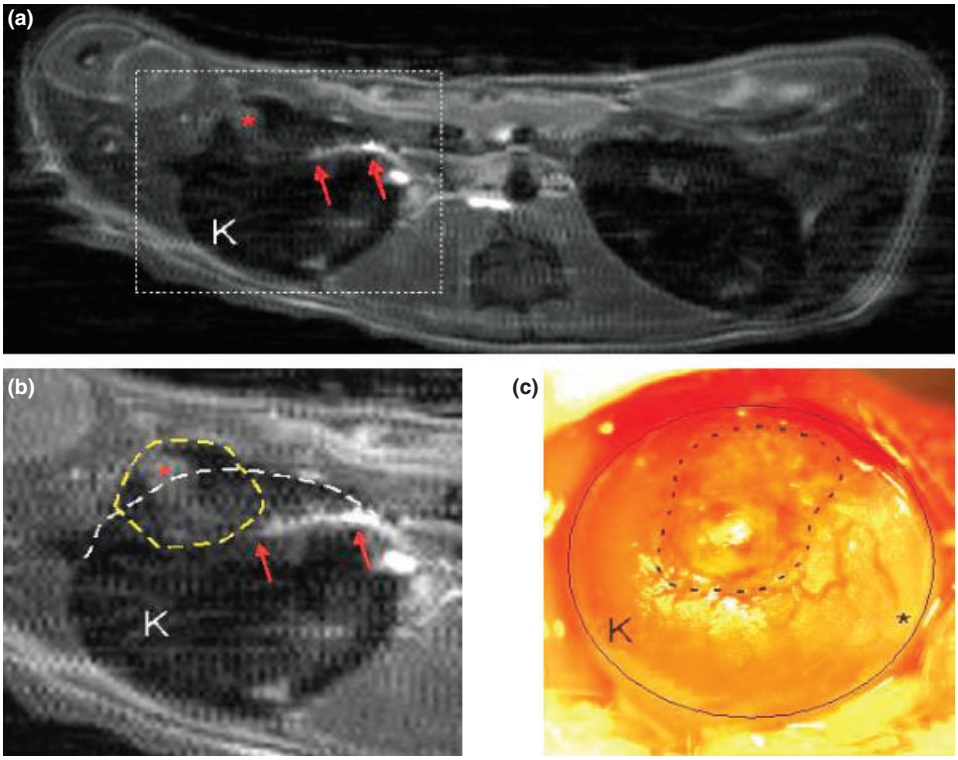

Figure 2 Representative imaging of vascularization of iron-labeled islet grafts on day 14. (a) Postcontrast magnetic resonance imaging (MRI) at day 14 shows a contrast-enhancement (red arrows) in the vicinity of labeled transplanted islets. Similar densities were not observed in the contralateral kidney. (b) Expanded view of 'A' revealing selective enhancement (asterisk) within the islets (dotted line) and the linear density (possibly a communicating vessel) (arrows). (c) Following MRI, the kidney (circle) was exposed *in vivo* and a low power photomicrograph was taken of the transplanted islets (dotted line). Note the blood vessels on the kidney surface near the transplant (a, b, and c are from the same kidney).

It has been previously reported that up to 60% of transplanted islets undergo apoptosis following transplantation [2]. Evaluation of T2 values and volumetric islet analysis did not show significant differences between day 3 and day 14. These findings suggest that iron labeling of islets can be used to localize islet grafts through noninvasive *in vivo* MRI, but may not alone be optimal for monitoring hemodynamic changes of islets after transplantation. As far as islet volume assessment, negative signals from the islet volumes are confirmed with T1 and Gd injection. The negative signals are relative changes in islet volume that allow extraction of islet volumes. Although this is a valid method, the study focus was on relative changes in, rather than definitive, islet volumes.

In this study, we showed that transplanted islets could be visualized on day 3 without labeling by contrast MRI. To our knowledge, this is the first demonstration of the use of systemic contrast agent injection (30 min before imaging) to detect unlabeled islet grafts by MRI. Increased T2 values (seen in islet grafts relative to kidney and muscle) typically reflect increased proton (water) relaxation. This suggests either edema or increased vessel permeability in the graft vicinity compared with other organs.

This approach focuses on increased post-transplant vascularization, and it remains to be tested whether this translates into, or correlates with, enhanced islet number and/or function.

We and others have shown a temporal evolution of new vessel formation in islet grafts using immunohistochemistry [19,26]. On post-transplant day 3 in this study, observed signal enhancement at the transplant site may result from leakage of contrast in newly formed blood vessels. No similar enhancement was observed in the surrounding kidney tissue possibly because of rapid clearance of gadolinium from pre-existing intact blood vessels. Contrast enhancement around islet grafts could also be seen at later stages of transplantation (beyond 14 days, preliminary data not shown). These findings may reflect proportional variations in permeability and vascular density in islet grafts on days 3,14, and beyond. In the course of the current study, a region of contrast enhancement consistent with a blood vessel was seen connecting the graft to the host tissue. If concomitant microscopy

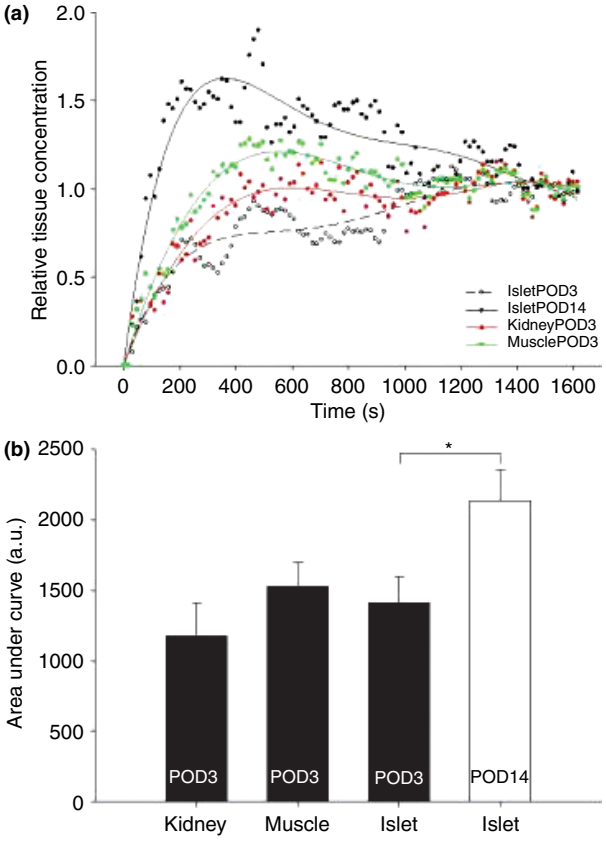

Figure 3 Normalized dynamic contrast-enhanced (DCE) magnetic resonance imaging gadolinium concentration curves at day 3 and 14. (a) At day 3, muscle and kidney contrast enhancement curves reached a peak in about 22 min, and a plateau by 30 min after contrast injection. Day 3 islet enhancement curve peak occurred at 21 min after injection. At day 14, islet curve peak is within 9 min of injection with a slow decline to similar levels as muscle and kidney by 30 min. (b) Area under the curve represents the relative amount of tissue contrast present during the 30-min DCE experiment. At day 3, all the tissues of interest had similar areas under the curve. At day 14, there was a significant increase in the area under the curve for islets compared to day 3. $*P < 0.05$.

confirms vascular nature, this may provide radiologic evidence for islet graft revascularization of host origin [27]. Donor islet endothelial cells also reportedly participate in neovascularization of islet grafts [28,29]. This study does not adequately address the source of neovascularization within islet grafts. However, our approach may be suitable for such studies particularly if donor mouse endothelial cells were co-transplanted [30].

Vascularization from the host kidney combined with vasculature from within the islets provides a conduit for contrast circulation systemically within the transplant site. This was demonstrated by our observations of contrast-enhanced blood vessels in the vicinity of islet grafts on day 14 (Fig. 2). Further support for this notion is provided by the rapid contrast enhancement on day 14, but not on day 3. However, enhancement within the islets is likely dependent on the number of healthy transplanted islets, their subsequent revascularization, and the number of known and unknown graft–host interactions.

A potential but unexplored question is whether Feridex labeling of islets results in loss of gadolinium-DTPA signal within the region of interest. While there are no published studies, to our knowledge, of mutually adverse effects between these two agents, some studies have noted altered sensitivity of MR signals in clinical settings [31].

These data are presented as a pilot study for a concept, which may apply to other organ transplants. A main limitation of our study from a diabetes point of view is that it addresses islet transplantation in a site that is not used clinically at present as the liver is currently the most successful site for clinical islet transplantation. However, it is likely that the field will shift to alternate islet transplant sites in the near future, especially in view of the inevitable resultant ischemia from portal vein injection of islets. Given the impact of enhanced vascularization on islet function [19,20], development and testing of therapeutic interventions in islet transplantation may greatly benefit from DCE MRI. This technique may also be of value in experimental or clinical organ transplantation.

Authorship

EH wrote the manuscript and designed and supervised the work. LS helped in designing the study. RW helped with imaging work. AT helped with islet labeling. JM, RP and RC helped with the overall project, AO supervised MRI work and helped in writing MRI portion.

Acknowledgements

This work was supported by the National Institutes of Health, NIH/NIDDK grant number 1-R01-DK077541-01. The content is solely the responsibility of the authors and does not necessarily represent the official views of the NIH or NIDDK. Technical assistance was provided by Gang Miao.

References

1. Ryan EA, Lakey JR, Paty BW, *et al.* Successful islet transplantation: continued insulin reserve provides long-term glycemic control. *Diabetes* 2002; **51**: 2148.
2. Davalli AM, Ogawa Y, Ricordi C, Scharp DW, Bonner-Weir S, Weir GC. A selective decrease in the beta cell mass

of human islets transplanted into diabetic nude mice. *Transplantation* 1995; **59**: 817.
3. Shapiro AM, Ryan EA, Lakey JR. Diabetes. Islet cell transplantation. *Lancet*. 2001; **358** (Suppl.): S21.
4. Carlsson PO, Palm F, Andersson A, Liss P. Markedly decreased oxygen tension in transplanted rat pancreatic islets irrespective of the implantation site. *Diabetes* 2001; **50**: 489.
5. Wang W, Upshaw L, Strong DM, Robertson RP, Reems J. Increased oxygen consumption rates in response to high glucose detected by a novel oxygen biosensor system in non-human primate and human islets. *J Endocrinol* 2005; **185**: 445.
6. Evgenov NV, Medarova Z, Dai G, Bonner-Weir S, Moore A. In vivo imaging of islet transplantation. *Nat Med* 2006; **12**: 144.
7. Jirak D, Kriz J, Herynek V, *et al.* MRI of transplanted pancreatic islets. *Magn Reson Med* 2004; **52**: 1228.
8. Koblas T, Girman P, Berkova Z, *et al.* Magnetic resonance imaging of intrahepatically transplanted islets using paramagnetic beads. *Transplant Proc* 2005; **37**: 3493.
9. Berkova Z, Kriz J, Girman P, *et al.* Vitality of pancreatic islets labeled for magnetic resonance imaging with iron particles. *Transplant Proc* 2005; **37**: 3496.
10. Turvey SE, Swart E, Denis MC, *et al.* Noninvasive imaging of pancreatic inflammation and its reversal in type 1 diabetes. *J Clin Invest* 2005; **115**: 2454.
11. Paty BW, Bonner-Weir S, Laughlin MR, McEwan AJ, Shapiro AM. Toward development of imaging modalities for islets after transplantation: insights from the National Institutes of Health Workshop on Beta Cell Imaging. *Transplantation* 2004; **77**: 1133.
12. Cuenod CA, Fournier L, Balvay D, Guinebretiere JM. Tumor angiogenesis: pathophysiology and implications for contrast-enhanced MRI and CT assessment. *Abdom Imaging* 2006; **31**: 188.
13. Cartwright L, Farhat WA, Sherman C, *et al.* Dynamic contrast-enhanced MRI to quantify VEGF-enhanced tissue-engineered bladder graft neovascularization: pilot study. *J Biomed Mater Res A* 2006; **77**: 390.
14. Medved M, Karczmar G, Yang C, *et al.* Semiquantitative analysis of dynamic contrast enhanced MRI in cancer patients: variability and changes in tumor tissue over time. *J Magn Reson Imaging* 2004; **20**: 122.
15. Rehman S, Jayson GC. Molecular imaging of antiangiogenic agents. *Oncologist* 2005; **10**: 92.
16. Brekke C, Lundervold A, Enger PO, *et al.* NG2 expression regulates vascular morphology and function in human brain tumours. *Neuroimage* 2006; **29**: 965.
17. Cheng HL, Chen J, Babyn PS, Farhat WA. Dynamic Gd-DTPA enhanced MRI as a surrogate marker of angiogenesis in tissue-engineered bladder constructs: a feasibility study in rabbits. *J Magn Reson Imaging* 2005; **21**: 415.
18. Rissanen TT, Korpisalo P, Markkanen JE, *et al.* Blood flow remodels growing vasculature during vascular endothelial growth factor gene therapy and determines between capillary arterialization and sprouting angiogenesis. *Circulation* 2005; **112**: 3937.
19. Miao G, Ostrowski RP, Mace J, *et al.* Dynamic production of hypoxia-inducible factor-1alpha in early transplanted islets. *Am J Transplant* 2006; **6**: 2636.
20. Miao G, Mace J, Kirby M, *et al.* In vitro and in vivo improvement of islet survival following treatment with nerve growth factor. *Transplantation* 2006; **81**: 519.
21. Eidt S, Kendall EJ, Obenaus A. Neuronal and glial cell populations in the piriform cortex distinguished by using an approximation of q-space imaging after status epilepticus. *AJNR Am J Neuroradiol* 2004; **25**: 1225.
22. Tofts PS. Modeling tracer kinetics in dynamic Gd-DTPA MR imaging. *J Magn Reson Imaging* 1997; **7**: 91.
23. Evgenov NV, Medarova Z, Pratt J, *et al.* In vivo imaging of immune rejection in transplanted pancreatic islets. *Diabetes* 2006; **55**: 2419.
24. Kriz J, Jirak D, Girman P, *et al.* Magnetic resonance imaging of pancreatic islets in tolerance and rejection. *Transplantation* 2005; **80**: 1596.
25. Tai JH, Foster P, Rosales A, *et al.* Imaging Islets Labeled With Magnetic Nanoparticles at 1.5 Tesla. *Diabetes* 2006; **55**: 2931.
26. Cao R, Eriksson A, Kubo H, Alitalo K, Cao Y, Thyberg J. Comparative evaluation of FGF-2-, VEGF-A-, and VEGF-C-induced angiogenesis, lymphangiogenesis, vascular fenestrations, and permeability. *Circ Res* 2004; **94**: 664.
27. Vajkoczy P, Olofsson AM, Lehr HA, *et al.* Histogenesis and ultrastructure of pancreatic islet graft microvasculature. Evidence for graft revascularization by endothelial cells of host origin. *Am J Pathol* 1995; **146**: 1397.
28. Nyqvist D, Kohler M, Wahlstedt H, Berggren PO. Donor islet endothelial cells participate in formation of functional vessels within pancreatic islet grafts. *Diabetes* 2005; **54**: 2287.
29. Brissova M, Fowler M, Wiebe P, *et al.* Intraislet endothelial cells contribute to revascularization of transplanted pancreatic islets. *Diabetes* 2004; **53**: 1318.
30. Anderson SA, Glod J, Arbab AS, *et al.* Noninvasive MR imaging of magnetically labeled stem cells to directly identify neovasculature in a glioma model. *Blood* 2005; **105**: 420.
31. Macarini L, Marini S, Milillo P, Vinci R, Ettorre GC. Double-contrast MRI (DC-MRI) in the study of the cirrhotic liver: utility of administering Gd-DTPA as a complement to examinations in which SPIO liver uptake and distribution alterations (SPIO-LUDA) are present and in the identification and characterisation of focal lesions. *Radiol Med (Torino)* 2006; **111**: 1087.

